

Date of publication xxxx 00, 0000, date of current version xxxx 00, 0000.

Digital Object Identifier 10.1109/ACCESS.2017.DOI

# A semi-automatic numerical algorithm for Turing patterns formation in a Reaction-Diffusion model

ROSANNA CAMPAGNA<sup>1</sup>, SALVATORE CUOMO<sup>1</sup>, FRANCESCO GIANNINO<sup>2</sup> and GERARDO SEVERINO<sup>2</sup>.

<sup>1</sup>Department of Mathematics and Applications

University of Naples Federico II, Italy (e-mail: rosanna.campagna@unina.it; salvatore.cuomo@unina.it)

<sup>2</sup>Department of Agricultural Sciences

University of Naples Federico II, Italy (e-mail: giannino@unina.it; gerardo.severino@unina.it)

Corresponding authors: Rosanna Campagna, Salvatore Cuomo (e-mail: {rosanna.campagna, salvatore.cuomo}@unina.it).

This work was supported by the grant "Programma di finanziamento della ricerca di Ateneo 2015" of the University of Naples Federico II, Italy.

**ABSTRACT** The Turing pattern formation is modeled by *reaction-diffusion* (RD) type *partial differential equations* (PDEs), and it plays a crucial role in ecological studies. Big data analytics and suitable frameworks to manage and predict structures and configurations are mandatory. The processing and resolution procedures of mathematical models relies upon numerical schemes, and concurrently upon the related automated algorithms. Starting from a RD model for vegetation patterns, we propose a semi-automatic algorithm based on a smart numerical criterion for observing ecological reliable results. Numerical experiments are carried out in the case of spot's formations.

**INDEX TERMS** Vegetation Turing patterns, finite difference methods, Internet of Things.

## I. INTRODUCTION

The availability of modeling frameworks to investigate biological [1], and environmental [2]–[4] phenomena is of paramount importance for predicting purposes. The huge amount of data from the real world also requires techniques and tools to extract, manage and properly classify information. The *Internet of Things* (IoT) system of connecting machines and sensors is a useful tool for reading the real world. In fact, by extracting information from a large number of data acquired in biological as well as environmental contexts, one gains physical insights on the processes at stake, and can forecast at different temporal/spatial scales. The basis of these approaches is the automation of the processing and resolution procedures of mathematical models that describe the real world. The Turing pattern formation is mathematically modelled by RD-type PDEs. Most of the early studies on Turing patterns dealt with chemical RD-systems. The fundamental concept introduced by Turing was that, in order to be stable (steady), states have to be diffusion-free. To the contrary, diffusion favors the emergence of unstable and spatially heterogeneous patterns [5]. The pattern formation dynamics generally occurs due to the interaction of two (or

more) chemicals. This is generally modelled by a system of nonlinear PDEs.

There are many studies relating biological processes to Turing patterns via RD models [6]. Due to the nonlinear nature of the overall mathematical problem, it is generally very hard getting an analytical solution. Thus, in the majority of the real world situations, one must resort to numerical methods. Nevertheless, there is a relatively limited number of studies on the matter, the importance of the problem at stake, notwithstanding. The widely adopted numerical schemes for RD models are the *finite difference* (FD) [7], and finite element methods [8]. More recently, discontinuous Galerkin finite element methods [9], [10] have become increasingly popular, as well. Finally, implicit-explicit schemes have been also used, especially in conjunction with spectral methods in Fluidmechanics [11]. One of the first example arising Turing instability is from the Brusselator model [12]. The unique feature of such a problem is that it enables one getting analytical solutions which lend themselves as benchmark to validate more involved numerical schemes [13]–[16]. The same is for the Schnakenberg model [17], representing a simplified version of the previous one [18], [19]. A detailed

analysis about the time-integration schemes, and numerical results can be found in [18]- [19]. Finally, a generalization of the previous models, accounting for the spatial pattern's distribution, was provided by Gray-Scott [20]. Implicit-explicit schemes to describe pattern formation arising from such a model can be found in [21]. Besides the numerical approaches, RD-type models related to Turing's patterns have been tackled by means of the cellular automata models [22]. Such an approach could be used to develop a counterpart to simulate both the Brusselator's model and that of Gray-Scott [23].

In this paper we present a numerical (FD) approach for a RD model describing the vegetation patterns' formation as determined by the interactions between biomass evolution, water availability and toxicity in plant-soil feedback [6], [24]. It is shown that our algorithm leads to a simple stability criterion avoiding numerical artifacts. In particular, such a criterion serves as a tool to be (consciously) used in the integration scheme in order to avoid meaningless results [25]. The paper is organized as follows. In the section II we present the RD model giving rise to the vegetation patterns formation; in section III we focus on the numerical solution by a FD scheme, and the accuracy vs stability of the numerical model. Section IV exploits the algorithmic into details; conclusions are outlined in the Section V.

## II. THE MATHEMATICAL MODEL AND THE DISCRETIZED SCHEME

We consider the numerical solution of the following system of nonlinear PDEs [24]:

$$\frac{\partial B}{\partial t} = D_B \Delta B + G_B(B, W, T), \quad (1a)$$

$$\frac{\partial W}{\partial t} = D_W \Delta W + G_W(B, W), \quad (1b)$$

$$\frac{\partial T}{\partial t} = T[Bqs - (k + wp)] + qdB, \quad (1c)$$

where  $B, W, T$  are the specific (per unit surface) biomass, water, and toxic compounds. The coefficients  $D_B, D_W \in \mathbb{R}^+$  accounts for the diffusion of the biomass and water, respectively, whereas the nonlinear reaction terms  $G_B$  and  $G_W$  are defined as:

$$\begin{aligned} G_B(B, W, T) &= cB^2W - (d + sT)B, \\ G_W(B, W) &= p - rB^2W - lW. \end{aligned} \quad (2)$$

The positive parameters appearing into (2) are chosen either in accordance with [26], [27] or selected from within an order-of-magnitude feasibility range [28], [29]. More precisely,  $p$  is the rain intensity,  $k$  is the rate of decay of toxicity, and  $s$  is the sensitivity of the plants to the toxicity (see Table 1 in [6], [24] for further details). Equations (1a)-(1c) are defined on a bounded domain  $\Omega \subset \mathbb{R}^2$ , and are subjected to zero Neumann-type boundary conditions along the boundary  $\partial\Omega$  of the domain. The initial conditions are:

$$B(x, y, 0) = B_0, \quad W(x, y, 0) = W_0, \quad T(x, y, 0) = 0, \quad (3)$$

for  $(x, y) \in \Omega$ . A FD scheme on a regular grid in Cartesian coordinates provides an approximation of the solution over a finite number of grid points  $\{z_{i,j}\}$ , s.t.  $z_{i,j} = (i\Delta x, j\Delta y)$   $i = 0, \dots, N_x - 1, j = 0, \dots, N_y - 1$ , with  $\Delta x := \frac{x_{max}}{N_x - 1}$  and  $\Delta y := \frac{y_{max}}{N_y - 1}$  the grid mesh-sizes. If a temporal grid is defined as  $\tau^k := k\Delta t$ ,  $k = 0, \dots, M$ , with temporal step-size  $\Delta t := \frac{t_{max}}{M}$ , the scheme provides an approximation, say  $u_{i,j}^k$ , at  $z_{i,j}$  and time step  $\tau^k$ .

Let  $u_{i,j}^k$  be the approximation of  $B, W$  and  $T$  at  $z_{i,j}$  and time step  $\tau^k$ . For the eqs (1a)-(1b) we apply a FD scheme forward in time and centered (second order) in the space, whereas (1c) is solved by a first order accurate forward Euler scheme. We then define a weight average scheme can be defined for the two PDEs, that is based on a convex ( $\theta$ -type) combination of the spatial terms of the forward/backward difference methods. We set  $D \equiv D_B = D_W$  in (1a)-(1b), so that it yields

$$\begin{aligned} u_{i,j}^{k+1} - u_{i,j}^k &= D\mu[\theta_1(\Delta y^2 \cdot \delta_x^2 u_{i,j}^{k+1} + \Delta x^2 \cdot \delta_y^2 u_{i,j}^{k+1}) + \\ &+ (1 - \theta_1)(\Delta y^2 \cdot \delta_x^2 u_{i,j}^k + \Delta x^2 \cdot \delta_y^2 u_{i,j}^k)] + \\ &+ \Delta t[\theta_2 g^{k+1} + (1 - \theta_2)g^k] \end{aligned} \quad (4)$$

$\forall (i, j), i = 1, \dots, N_x, j = 1, \dots, N_y$ , being

$$\delta_x^2 u_{i,j}^k = u_{i+1,j}^k - 2u_{i,j}^k + u_{i-1,j}^k,$$

$$\delta_y^2 u_{i,j}^k = u_{i,j+1}^k - 2u_{i,j}^k + u_{i,j-1}^k,$$

whereas  $g^k$  is the non linear term at the time level  $\tau^k$ , and

$$\mu = \frac{\Delta t}{\Delta x^2 \Delta y^2}. \quad (5)$$

To investigate the Turing pattern formation, it is sufficient to assume  $\theta_2 = 0$  (explicit scheme).

## III. A SEMI-AUTOMATIC ALGORITHM FOR VEGETATION TURING PATTERNS

With  $\theta := \theta_1$ , we re-write (4) into matrix form as  $AX = Y$ , being  $A, X$  and  $Y$  a  $3N_x N_y \times 3N_x N_y$  matrix, and  $3N_x N_y \times N_x N_y$  matrices, respectively. Such matrices are defined as:

$$A = \begin{pmatrix} A_B & 0 & 0 \\ 0 & A_W & 0 \\ 0 & 0 & I_{N_x \times N_y} \end{pmatrix},$$

$$X = \begin{pmatrix} X_B^{k+1} \\ X_W^{k+1} \\ X_T^{k+1} \end{pmatrix},$$

$$Y = \begin{pmatrix} Y_B^k \\ Y_W^k \\ Y_T^k \end{pmatrix},$$

where  $A_B$  and  $A_W$  are square sparse, pentadiagonal, non-symmetric, positive definite, diagonally dominant, and banded (width  $N_x$ ) matrices of  $N_x \times N_y$ -order;  $I_{N_x \times N_y}$  is the unit matrix of order  $N_x \times N_y$ . By setting

$$\begin{aligned} R_1 &:= \frac{\theta \Delta t D_B}{(\Delta x)^2}, \quad R_2 := \frac{\theta \Delta t D_B}{(\Delta y)^2}, \\ r_1 &:= \frac{(1 - \theta) \Delta t D_B}{(\Delta x)^2}, \quad r_2 := \frac{(1 - \theta) \Delta t D_B}{(\Delta y)^2}, \end{aligned} \quad (6)$$

and

$$\begin{aligned} S_1 &:= \frac{\theta \Delta t D_W}{(\Delta x)^2}, & S_2 &:= \frac{\theta \Delta t D_W}{(\Delta y)^2}, \\ s_1 &:= \frac{(1-\theta) \Delta t D_W}{(\Delta x)^2}, & s_2 &:= \frac{(1-\theta) \Delta t D_W}{(\Delta y)^2}. \end{aligned} \quad (7)$$

( $k > 0$ ), the  $(i, j)$ -th elements of  $A_B$  and  $A_W$  are respectively:

$$\begin{aligned} (1 + 2R_1 + 2R_2)b_{i,j}^{k+1} &- R_1 (b_{i+1,j}^{k+1} + b_{i-1,j}^{k+1}) + \\ &- R_2 (b_{i,j-1}^{k+1} + b_{i,j+1}^{k+1}) \end{aligned} \quad (8)$$

and

$$\begin{aligned} (1 + 2S_1 + 2S_2)w_{i,j}^{k+1} &- S_1 (w_{i+1,j}^{k+1} + w_{i-1,j}^{k+1}) + \\ &- S_2 (w_{i,j-1}^{k+1} + w_{i,j+1}^{k+1}) \end{aligned} \quad (9)$$

( $i = 0, \dots, N_x - 1, j = 0, \dots, N_y - 1$  and  $k = 0, \dots, M$ ). Likewise, the  $Y$ -blocks are

$$\begin{aligned} Y_B^k &= b_{i,j}^k + \Delta t \left[ cb_{i,j}^k w_{i,j}^k - (d + st_{i,j}^k)b_{i,j}^k \right] + \\ &+ r_1 (b_{i+1,j}^k - 2b_{i,j}^k + b_{i-1,j}^k) + \\ &+ r_2 (b_{i,j-1}^k - 2b_{i,j}^k + b_{i,j+1}^k) \end{aligned} \quad (10)$$

$$\begin{aligned} Y_W^k &= w_{i,j}^k + \Delta t \left[ p - rb_{i,j}^k w_{i,j}^k - lw_{i,j}^k \right] \\ &+ s_1 (w_{i+1,j}^k - 2w_{i,j}^k + w_{i-1,j}^k) + \\ &+ s_2 (w_{i,j-1}^k - 2w_{i,j}^k + w_{i,j+1}^k) \end{aligned}$$

and

$$Y_T^k = t_{i,j}^k + \Delta t \left[ q(d + st_{i,j}^k)b_{i,j}^k - (k + wp)t_{i,j}^k \right]$$

( $i = 0, \dots, N_x - 1, j = 0, \dots, N_y - 1$ ). The parameter  $\theta$  allows to swap the numerical scheme, that is  $\theta = 0$  provides explicit (forward in time) FD,  $\theta = 1/2$  corresponds to the Crank-Nicolson scheme, whereas  $\theta = 1$  a fully implicit (backward in time) Euler scheme. The explicit scheme has second-order convergence in the space, and a first order accuracy in time. It is conditionally stable, and the Courant-Friedrichs-Lewy (CFL) condition is:

$$\exists c > 0 : \Delta t \leq c \Delta x^2.$$

For the numerical approximation (4), the CFL writes as

$$\exists c > 0 : \Delta t \leq \frac{c}{2D} \frac{\Delta x^2 \Delta y^2}{\Delta x^2 + \Delta y^2}. \quad (11)$$

Given this, we aim at:

- (1) keeping low the truncation error;
- (2) containing the round-off error propagation, and therefore the sneaky numerical artefacts which can arise when  $D\mu(\Delta x^2 + \Delta y^2) \rightarrow 0$ .

TABLE 1: Semi-automatic algorithm for Turing pattern

**Require:** Set input values {under hypothesis (11)}

- 1: **for**  $k = 1 : t_{max}$  **do**
- 2: Computation of  $Y_B^k$  by  $D_B, c, d, s, \Delta t, r_1, r_2$
- 3: Computation of  $Y_W^k$  by  $D_W, p, r, \Delta t, s_1, s_2$
- 4: Computation of  $Y_T^k$  by  $\Delta t, q, d, s, w, k, p$
- 5: Solve  $A_B[X_B^{k+1}] = Y_B^k$  {call *GMRES*}
- 6: Solve  $A_W[X_W^{k+1}] = Y_W^k$  {call *GMRES*}
- 7: Solve  $I_{N_x \times N_y}[X_T^{k+1}] = Y_T^k$  {*T* updating}
- 8: **end for**
- 9: **return**

TABLE 2: Numerical results.

case num.	(11) satisfied	$\Delta t$	$\frac{\Delta x}{\Delta y}$	$\Phi$	$\ B - B_{ref}\ _\infty$
1)	yes	0.05	0.5	0.079	-
2)	no	0.05	0.38	0.046	GMRES tol. not satisfied
3)	no	0.08	0.5	0.079	4.8115e+01
4)	no	0.09	0.5	0.079	numerically singular matrices
5)	no	0.1	0.5	0.079	numerically singular matrices

#### IV. RESULTS

Due to the block diagonal form and the constant coefficients of  $A_B$ ,  $A_W$  and  $I_{N_x \times N_y}$ , we solve w.r.t.  $B$ ,  $W$  and  $T$  independently at each time level. Each system is solved (see Table 1) by the *generalized minimal residual iterative method* (GMRES). With the parameter values listed in the Table 1 of [24], simulations were performed on a  $N_x \times N_y = 100 \times 100$  square lattice with  $x_{max} = 50$ , and  $y_{max} = 50$ . The initial conditions are  $B_0 = 0.2 \text{ kg/m}^2$  in  $N_0 = 5000$  randomly selected elements, and  $B_0 = 0$  in the remaining nodes,  $W_0 = 40 \text{ kg/m}^2$  and  $T_0 = 0$  at all points. Moreover we fix  $p = 0.8$  and we run the simulations along  $t_{max} = 20000$  days. We set  $\theta = 0$  and

$$\Phi = \frac{c}{2D} \frac{\Delta x^2 \Delta y^2}{\Delta x^2 + \Delta y^2}$$

in the (11), with  $c = 1$  and

$$\frac{1}{D} = \min \left\{ \frac{1}{DB}, \frac{1}{DW} \right\}.$$

Table 2 summarizes the results obtained for different values of  $\Delta t$ ,  $\Delta x = \Delta y$  and  $\Phi$ ; a brief description follows.

**Test case condition satisfied:**  $\Delta t < \Phi$

case 1) Let be  $\Delta t = 0.05$ ,  $\Delta x = \Delta y = 0.5$ ,  $\Phi = 0.0797$ . The condition (11) is satisfied and we assume the computed solution  $B_{ref}$  as a reference. The last column of Table 2 refers to the maximum error in the solution, w.r.t.  $B_{ref}$ . In the Fig.1 (up row) we have depicted the temporal evolution of the biomass-density, whereas the temporal evolution of biomass density, averaged over the lattice is represented in the Fig. 2 (left). The response of plants to toxicity negative feedback ( $s = 0.2$ ) combined

with a high toxicity decay rate ( $k = 0.2$ ), gives rise (after about 12 minutes) to stable patterns.

### Test cases condition not satisfied: $\Delta t > \Phi$

In the Table 2 we have summarized also the results obtained on failing the condition (11), both by increasing  $\Delta t$  and decreasing  $\Phi$ :

case 2) Let be  $\Delta t = 0.05$ ,  $\Delta x = \Delta y = 0.38$ ,  $\Phi = 0.0469$ . A reduction of  $\Delta x = \Delta y$ , does not let  $\Phi$  to overcome  $\Delta t$ , and concurrently the condition (11) is violated. With the parameters values listed in the first line of the Table 2, GMRES (without restart and in the default number equal to 10 iterations) doesn't satisfy the prescribed tolerances  $\epsilon \in \{10^{-6}, 10^{-4}, 10^{-2}\}$ ; the execution is interrupt since the solver GMRES doesn't converge.

case 3) Let  $\Delta t = 0.08$ ,  $\Delta x = \Delta y = 0.5$ ,  $\Phi = 0.0797$ . By increasing  $\Delta t$  w.r.t.  $\Phi$ , the computed values move away from the reference values, according to the absolute error in the last column. In Fig.1 (down) some spots represent the biomass evolution when the condition (11) is violated. The disappearance of the pattern formation after about 10 seconds, is due to the amplification of the round-off errors through the time stepping, and it demonstrates that also a small perturbation in the amplification factor can lead to an unreliable solution. The Fig.2 (right) shows how the mean value of the biomass vanishes (in about 7000 time steps).

case 4), 5) Let us assume that  $\Delta t = 0.09$  and  $\Delta t = 0.1$ , with  $\Delta x = \Delta y = 0.5$  and  $\Phi = 0.0797$ . An increase of  $\Delta t$  renders the iteration matrices (quasi)-singular, such that no solution can be achieved.

## V. CONCLUSIONS

The IoT systems can be viewed as a glass for reading the real world, granting the process and producing a huge amount of data. The automation of the processing and resolution procedures of mathematical models describing the real world is mandatory to get insights on the physics underlying the biological/environmental processes.

In the present paper we have developed a numerical scheme for a particular RD model describing the formation and evolution of the vegetation pattern. The numerical scheme relies upon a semi-automatic algorithm based on a stability criterion, that limits the amplification error in the computed solution. Simulations show that, when the criterion is satisfied, the numerical scheme converges towards a reliable solution.

## ACKNOWLEDGMENT

This work was supported by the grant "Programma di finanziamento della ricerca di Ateneo 2015" of the University of Naples Federico II, Italy

## REFERENCES

- [1] G. Severino and D. M. Tartakovsky, "A boundary-layer solution for flow at the soil-root interface," *Journal of mathematical biology*, vol. 70, no. 7, pp. 1645–1668, 2015.
- [2] G. Severino, V. Monetti, A. Santini, and G. Toraldo, "Unsaturated transport with linear kinetic sorption under unsteady vertical flow," *Transport in porous media*, vol. 63, no. 1, pp. 147–174, 2006.
- [3] G. Severino, D. M. Tartakovsky, G. Srinivasan, and H. Viswanathan, "Lagrangian models of reactive transport in heterogeneous porous media with uncertain properties," *Proceedings of the Royal Society of London A: Mathematical, Physical and Engineering Sciences*, vol. 468, no. 2140, pp. 1154–1174, 2012.
- [4] G. Severino, S. De Bartolo, G. Toraldo, G. Srinivasan, and H. Viswanathan, "Travel time approach to kinetically sorbing solute by diverging radial flows through heterogeneous porous formations," *Water Resources Research*, vol. 48, no. 12, 2012, w12527.
- [5] A. M. Turing, "The chemical basis of morphogenesis," *Philosophical Transactions of the Royal Society of London B: Biological Sciences*, vol. 237, no. 641, pp. 37–72, 1952.
- [6] G. Severino, F. Giannino, F. Carteni, S. Mazzoleni, and D. M. Tartakovsky, "Effects of hydraulic soil properties on vegetation pattern formation in sloping landscapes," *Bulletin of Mathematical Biology*, 2017.
- [7] C. Pao, "Numerical solutions of reaction-diffusion equations with nonlocal boundary conditions," *Journal of Computational and Applied Mathematics*, vol. 136, no. 1, pp. 227–243, 2001.
- [8] L. Tobiska, "Johnson, c., numerical solution of partial differential equations by the finite element method. cambridge etc., cambridge university press 1988," *ZAMM - Journal of Applied Mathematics and Mechanics / Zeitschrift für Angewandte Mathematik und Mechanik*, vol. 71, no. 10, pp. 390–390, 1991.
- [9] J. Zhu, Y.-T. Zhang, S. A. Newman, and M. Alber, "Application of discontinuous galerkin methods for reaction-diffusion systems in developmental biology," *Journal of Scientific Computing*, vol. 40, no. 1, pp. 391–418, 2009.
- [10] D. A. Barajas-Solano and D. M. Tartakovsky, "Stochastic collocation methods for nonlinear parabolic equations with random coefficients," *SIAM/ASA J. Uncert. Quant.*, vol. 4, no. 1, pp. 475–494, 2016.
- [11] S. J. Ruuth, "Implicit-explicit methods for reaction-diffusion problems in pattern formation," *Journal of Mathematical Biology*, vol. 34, no. 2, pp. 148–176, 1995.
- [12] I. Prigogine and R. Lefever, "Symmetry breaking instabilities in dissipative systems. ii," *The Journal of Chemical Physics*, vol. 48, pp. 1695–1700, Feb. 1968.
- [13] F. Manaa SA; Saeed, RK; Easif, "Numerical solution of brusselator model by finite difference method," *Journal of Applied Sciences Research*, vol. 6, no. 11, pp. 1632–1646, 2010.
- [14] Z. U. A. Zafar, K. Rehan, M. Mushtaq, and M. Rafiq, "Numerical treatment for nonlinear brusselator chemical model," *Journal of Difference Equations and Applications*, vol. 23, no. 3, pp. 521–538, 2017.
- [15] R. Mittal and R. Jiware, "Numerical solution of two-dimensional reaction-diffusion brusselator system," *Applied Mathematics and Computation*, vol. 217, no. 12, pp. 5404 – 5415, 2011.
- [16] R. Mittal and R. Rohila, "Numerical simulation of reaction-diffusion systems by modified cubic b-spline differential quadrature method," *Chaos, Solitons & Fractals*, vol. 92, pp. 9 – 19, 2016.
- [17] J. Schnakenberg, "Simple chemical reaction systems with limit cycle behaviour," *Journal of Theoretical Biology*, vol. 81, no. 3, pp. 389 – 400, 1979.
- [18] I. Sgura, B. Bozzini, and D. Lacitignola, "Numerical approximation of turing patterns in electrodeposition by adi methods," *Journal of Computational and Applied Mathematics*, vol. 236, no. 16, pp. 4132 – 4147, 2012.
- [19] R. Zhang, X. Yu, J. Zhu, and A. F. Loula, "Direct discontinuous galerkin method for nonlinear reaction-diffusion systems in pattern formation," *Applied Mathematical Modelling*, vol. 38, no. 5, pp. 1612 – 1621, 2014.
- [20] P. Gray and S. Scott, "Autocatalytic reactions in the isothermal, continuous stirred tank reactor," *Chemical Engineering Science*, vol. 39, no. 6, pp. 1087 – 1097, 1984.
- [21] K. Zhang, J. C.-F. Wong, and R. Zhang, "Second-order implicit-explicit scheme for the gray-scott model," *Journal of Computational and Applied Mathematics*, vol. 213, no. 2, pp. 559–581, 2008.
- [22] C. P. Gravan and R. Lahoz-beltra, "Evolving morphogenetic fields in the zebra skin pattern based on turing's morphogen hypothesis," *Int. J. Appl. Math. Comput. Sci.*, vol. 14, no. 3, p. 351–361, 2004.

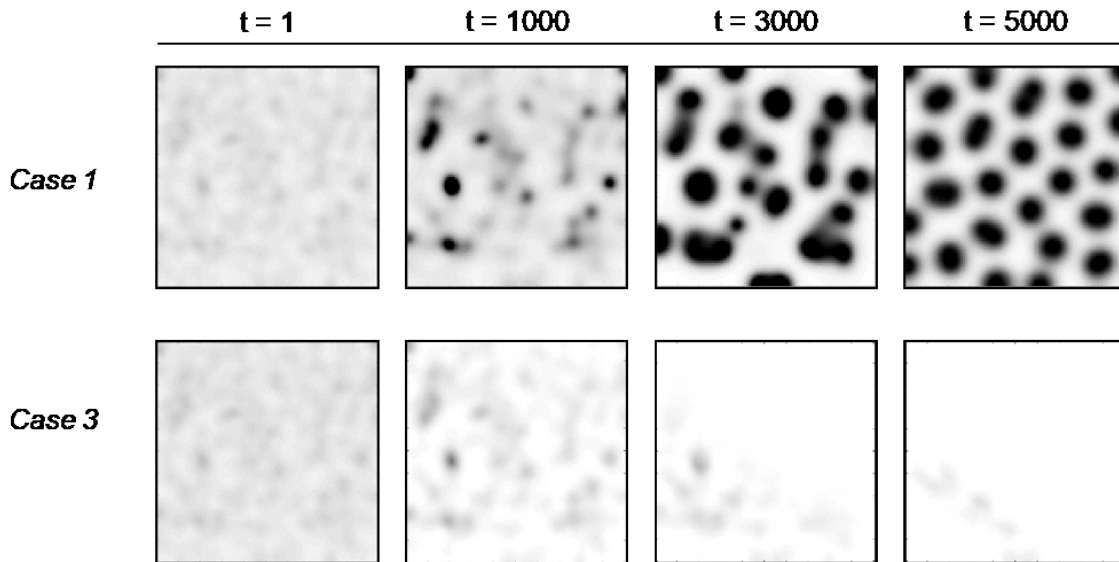


FIGURE 1: The temporal evolution of biomass density: case 1) in Table 2, with  $\Delta t = 0.05$ ,  $\Delta x = \Delta y = 0.5$ ,  $\Phi = 0.0797$  (up); case 3) in Table 2, with  $\Delta t = 0.08$ ,  $\Delta x = \Delta y = 0.5$ ,  $\Phi = 0.0797$  (down).

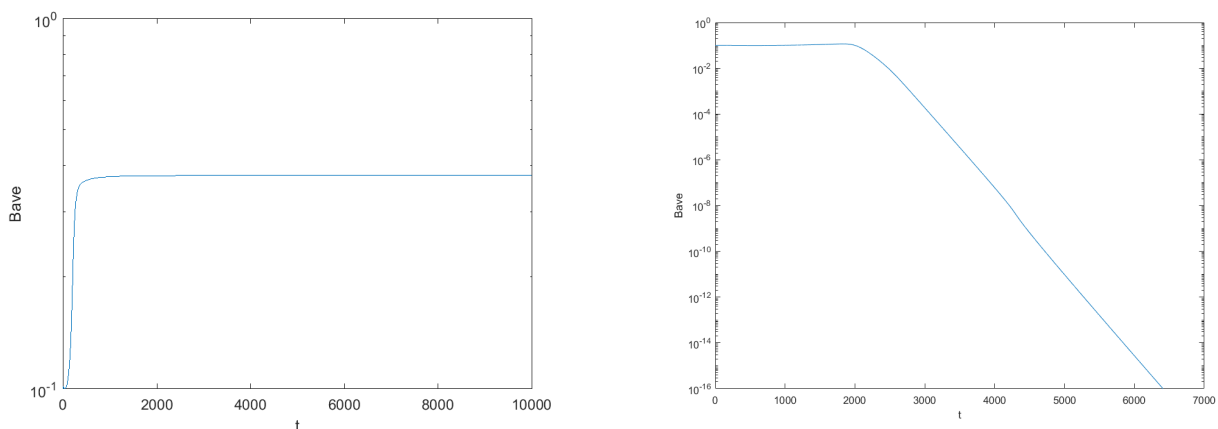


FIGURE 2: The temporal evolution of mean biomass density in case 1) (left) and case 3) (right). In this last case, the mean value decreases fast toward zero in less than 7000 time steps.

- [23] J. E. Pearson, "Complex patterns in a simple system," *Science*, vol. 261, no. 5118, pp. 189–192, 1993.
- [24] A. Marasco, A. Iuorio, F. Cartení, G. Bonanomi, D. M. Tartakovsky, S. Mazzoleni, and F. Giannino, "Vegetation pattern formation due to interactions between water availability and toxicity in plant–soil feedback," *Bulletin of Mathematical Biology*, vol. 76, no. 11, pp. 2866–2883, 2014.
- [25] R. Seppelt and O. Richter, "'it was an artefact not the result': A note on systems dynamic model development tools," *Environmental Modelling & Software*, vol. 20, no. 12, pp. 1543 – 1548, 2005, *environmental Knowledge and Information Systems*.
- [26] C. Klausmeier, "Regular and irregular patterns in semiarid vegetation," *Science*, 1999.
- [27] F. Cartení, A. Marasco, G. Bonanomi, S. Mazzoleni, M. Rietkerk, and F. Giannino, "Negative plant feedback explaining ring formation in clonal plants," *Journal of Theoretical Biology*, 2012.
- [28] S. Gómez, G. Severino, L. Randazzo, G. Toraldo, and J. Otero, "Identification of the hydraulic conductivity using a global optimization method," *agricultural water management*, vol. 96, no. 3, pp. 504–510, 2009.
- [29] A. Comegna, A. Coppola, V. Comegna, G. Severino, A. Sommella, and C. Vitale, "State-space approach to evaluate spatial variability of field measured soil water status along a line transect in a volcanic-vesuvian soil," *Hydrology and Earth System Sciences*, vol. 14, no. 12, pp. 2455–2463, 2010.



Rosanna Campagna . (Department of Mathematics and Applications “R. Caccioppoli”, University of Naples Federico II) Her research activity is concerned with the development and the analysis of numerical methods and computational approaches for the identification and parameter estimation of applied models. Theoretical and computational results are concerned with numerical methods for inverse problems, such as the Laplace transform inversion and the image restoration; she

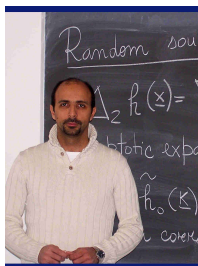
has worked in the software design for scientific computing and numerical methods for PDEs and related applications, including the biological-environmental modeling and the management of water systems.



Salvatore Cuomo (Department of Mathematics and Applications “R. Caccioppoli”, University of Naples Federico II). His research activity is concerned with the inverse problems, numerical methods and scientific computing algorithms. He also worked in the numerical problems in several application fields, including e-health and engineering. He is a member of several international and national research projects.



Francesco Giannino (Department of Agricultural Sciences, University of Naples Federico II) His research interest is mainly devoted to the design, development and analysis of mathematical models in biology. Methodological and computational aspects have been considered for several different applications. The research has been carried out in the frame of several international projects and collaborations with European research groups which are leaders in the area of biology modeling.



Gerardo Severino (Department of Agricultural Sciences, University of Naples Federico II). His research activity is concerned with the theory of flow and transport in heterogeneous porous formations; up-scaling of hydraulic properties; hydraulics of wells in randomly heterogeneous aquifers; soil hydrology; stochastic differential equations; inverse modelling. He serves as Associate Editor for numerous leading journals, and he has several ongoing research cooperations with

both national and international academic Institutions. He is member of several international and national research projects.

...